Separation Science and Technology
Publication details, including instructions for authors and subscription information:
http://www.informaworld.com/smpp/title~content=t713708471

Effect of Concentration Gradients in Barrier Separation Cells

Max E. Breuer[ab]; Karl Kammermeyer[a]
[a] Department of Chemical Engineering, University of Iowa, Iowa City, Iowa [b] Chemicals Division, Union Carbide Corporation, South Charleston, West Virginia

To cite this Article Breuer, Max E. and Kammermeyer, Karl(1967) 'Effect of Concentration Gradients in Barrier Separation Cells', Separation Science and Technology, 2: 3, 319 — 334
To link to this Article: DOI: 10.1080/01496396708049705
URL: http://dx.doi.org/10.1080/01496396708049705

SEPARATION SCIENCE, 2(3), 319–334 (1967)

Effect of Concentration Gradients in Barrier Separation Cells

MAX E. BREUER* and KARL KAMMERMEYER
DEPARTMENT OF CHEMICAL ENGINEERING, UNIVERSITY OF IOWA
IOWA CITY, IOWA

Summary

Concentration gradients in the gas phase above and below the barrier in separation cells were measured. The experimental data were compared with existing theories and none of the theories adequately correlated the data over the range of parameters studied. A new, geometry-dependent, theory was formulated. This theory, which allows for mixing by diffusion above and below the barrier, gave better predictions, both for product concentrations and for permeated flow rate, than any of the existing theories, and also predicts concentration profiles. Although the theoretical model was developed in a study of separation of gases, it could be applied to other systems as well, if the proper permeability and diffusion coefficients were used.

Mass transfer within separative barriers themselves has been studied extensively, both for porous and polymeric barriers. However, the mass transfer in the gas phase immediately adjacent to the surfaces of the barrier has received only limited, if any, attention. The concentration in this gas phase determines the driving forces for the flow through the barrier.

Several publications (*1,2,4,6–8*) have dealt with estimating the separation in the gas phase by making assumptions of perfect mixing, or of no mixing, on both sides of the barrier. In view of the low absolute permeabilities of presently available barriers and the resulting low flow rates, it is highly unlikely that perfect mixing will be achieved in any actual separation cell. Also, the assumptions

* Present address: Chemicals Division, Union Carbide Corporation, South Charleston, West Virginia.

made in the "no-mixing" case (II) of Weller and Steiner (7,8) would be difficult to achieve in practice. They assume that "the gas composition on the low pressure side is given by the relative rates of permeation of the individual constituents at that point." This assumption would be true only if the barrier were far enough away from the low-pressure flow stream that the gas composition of this stream did not affect the composition next to the barrier.

Oishi et al. (5) presented a theoretical analysis of a gaseous diffusion cell on the basis of the Weller and Steiner equations. The conclusion was reached that counterflow operation should give the greatest separation. Parallel laminar flow, and flow with mixing on both sides of the barrier, should give less separation (in that order).

Since it is unlikely that perfect mixing will occur in a separation cell, and since the assumptions made in previous no-mixing theories are somewhat unrealistic, it is necessary to consider a theory which recognizes the existence of a concentration gradient on the upstream side of the barrier, and which also allows for the flow stream on the downstream side of the barrier to be immediately adjacent to the barrier. In addition, any concentration gradient will have associated with it a diffusional flow, which can be thought of as a sort of mixing and which should be included in a theoretical model. The authors' formulation, in an attempt to achieve these goals, is as follows.

THEORY

Concentration gradients above and below the barrier can exist in three directions:

1. Parallel to the bulk flow of nonpermeated gas.
2. Perpendicular to the bulk flow and perpendicular to the barrier surface.
3. Perpendicular to the bulk flow and parallel to the barrier surface.

Effect 3 would be due to frictional effects at the cell wall and end effects at the feed and product ends of the cell. These effects will depend on the flow rate and the geometry of the cell. In view of the relatively low flow rates encountered in separation cells, effect 3 can be neglected.

Effect 2 will be due to depletion of the faster permeating component at the surface of the barrier. The existence of this "exhaustion layer" will depend upon the relative magnitudes of the gaseous-

phase diffusion coefficient, and the permeability coefficient for the system being studied. Binary gas diffusion coefficients are of the order of 1 cm²/sec-cm Hg, and permeability coefficients are of the order of 10^{-6} to 10^{-9}. Thus the resistance to flow caused by the barrier is many orders of magnitude larger than that caused by gaseous diffusion. Therefore effect 2 can be neglected. McAfee (3) states that an exhaustion layer will not form until the dimension between the barrier and the top of the cell is of the order of D_{AB}/K_P; then this dimension of the cell would be approximately 10^6 to 10^9 cm, a rather large cell, to say the least.

Thus the only concentration gradient to be considered is the one parallel to the bulk flow—effect 1. This concentration gradient is caused by the separative action of the barrier; the faster permeating component will be gradually depleted in the nonpermeated stream. The diffusional flow associated with this gradient will be accounted for.

A diagram of a schematic separation cell for the following derivation is shown in Fig. 1. A material balance can be written for component B around an incremental element from (l) to ($l + h$).

$$Q_B(l) + D_B(l) + q_B(l) + d_B(l) = Q_B(l+h) + D_B(l+h) + q_B(l+h) + d_B(l+h) \quad (1)$$

[All flows are in cm³(STP)/sec]

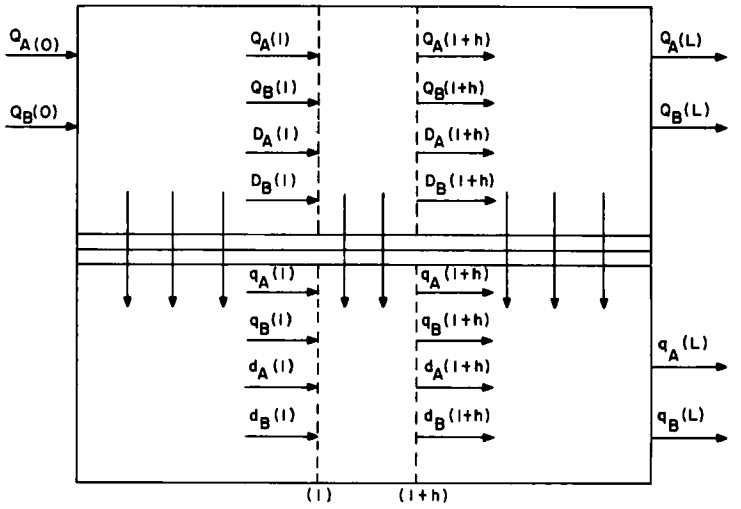

FIG. 1. Schematic separation cell.

After dividing Eq. (1) by h, rearranging, and taking the limit as $h \rightarrow 0$, we obtain

$$Q'_B + D'_B + q'_B + d'_B = 0 \tag{2}$$

where

$$Q'_B = \frac{dQ_B}{dl} \tag{3}$$

Similarly, for component A,

$$Q'_A + D'_A + q'_A + d'_A = 0 \tag{4}$$

A material balance written around the incremental element on the low-pressure side can be used to relate the change in q, d, and the flow permeating the barrier:

$$q_B(l+h) + d_B(l+h) - q_B(l) - d_B(l) = K_{PB}\frac{w}{t}h(P_H X_B - P_L Y_B) \tag{5}$$

Dividing both sides of Eq. (5) by h, rearranging, and taking the limit as $h \rightarrow 0$, we obtain

$$q'_B + d'_B = K_B\overline{DPB} \tag{6}$$

where

$$\overline{DPB} = (P_H X_B - P_L Y_B) \tag{7}$$

and

$$K_B = K_{PB}\frac{w}{t} \tag{8}$$

Similarly, for component A,

$$q'_A + d'_A = K_A\overline{DPA} \tag{9}$$

For the diffusional flow,

$$D_A = -K_{DH}X'_A \tag{10}$$

$$D_B = -K_{DH}X'_B \tag{11}$$

For a binary system,

$$X_A = 1 - X_B \tag{12}$$

Combining Eqs. (2), (6), and (11),

$$X'_B Q + X_B Q' - K_{DH}X''_B + K_B\overline{DPB} = 0 \tag{13}$$

Similarly, from Eqs. (4), (9), (10), and (12),

$$-X'_B Q + (1 - X_B)Q' + K_{DH}X''_B + K_A\overline{DPA} = 0 \tag{14}$$

Subtracting Eq. (13) from (14) and solving for X'_B we have

$$X'_B = (1/2Q)\ [K_A\overline{DPA} - K_B\overline{DPB} + (1 - 2X_B)Q'] + K_{DH}X''_B/Q \tag{15}$$

Adding Eqs. (13) and (14),

$$Q' = -K_A\overline{DPA} - K_B\overline{DPB} \tag{16}$$

There are now two equations, (15) and (16), with three unknowns, X_B, Y_B, and Q_B. A third equation can be obtained by an over-all material balance from $l = 0$ to $l = l$:

$$Q^f_B = Q_B + D_B + q_B + d_B \tag{17}$$

For the diffusion terms at any point,

$$D_B = -D_A \tag{18}$$

$$d_B = -d_A \tag{19}$$

Therefore

$$Q^f = Q + q \tag{20}$$

From Eqs. (17) and (20) we can obtain an expression for Y_B in terms of X_B and Q:

$$Y_B = (X^f_B Q^f - X_B Q)/(Q^f - Q) + (K_{DH}X'_B + K_{DL}Y'_B)/(Q^f - Q) \tag{21}$$

A straightforward analytical solution of Eqs. (15), (16), and (21) would be exceedingly difficult at best, and the authors have not been able to find one. However, the equations have been solved by numerical techniques.

If we ignore, for the time being, the terms involving the diffusion constants, Eqs. (15), (16), and (21) can be solved by a simple "crude Euler" stepping technique.

$$X_B(0) = X^f_B \tag{22}$$

$$Q(0) = Q^f \tag{23}$$

TABLE 1

Iteration Procedure for Plug Flow

Given:	(a) X_B^f, feed concentration
	(b) Q^f, feed flow rate
	(c) K_{PA}, K_{PB}, permeability coefficients of gases in mixture
	(d) Width, length, and thickness of barrier
	(e) h, incremental barrier length
Steps in *computer use:*	
	(1) Solve for Q' from Eq. (16)
	(2) Solve for X'_B from Eq. (15) omitting diffusion term (last term in equation)
	(3) $X_B(l+h) = X_B(l) + X'_B(l)h$
	(4) $Q(l+h) = Q(l) + Q'(l)h$
	(5) Solve for $Y_B(l+h)$ from Eq. (21) omitting diffusion term (last term)
	(6) Iterate steps (1) through (5) for the desired cell length

For $Y_B(0)$ we will use a perfect mixing approximation taking Y_B in equilibrium with X_B^f. The iteration procedure given in Table 1 is then used.

The solution obtained describes a simple plug flow, i.e., a unidirectional flow system. It differs from the no-mixing solution of Weller and Steiner (*7,8*) and Naylor and Backer (*4*) in that Y_B is a function of both Q and X_B, not of X_B alone.

The inclusion of the diffusional terms in Eqs. (15), (16), and (21) not only complicates the solution, but also introduces additional boundary conditions. The only diffusion which can occur at the cell walls, i.e., at $l = 0$ and $l = L$, is diffusion into and out of the feed supply and product takeoff tubes. Since the cross-sectional area of these tubes is small compared to the cross-sectional area of the cell, this diffusion can be neglected. The assumption of zero diffusion at the wall requires the following boundary conditions:

$$X'_B(0) = X'_B(L) = Y'_B(0) = Y'_B(L) = 0 \tag{24}$$

The value of $Q(0)$ is known (Q^f), but the value of $X_B(0)$ is not necessarily X_B^f. There will be a diffusional flow of component B toward the wall at $l = 0$, and since this flow stops at the wall, it will "build up" there, and increase the value of $X_B(0)$.

The equations with the diffusional terms cannot be solved in the same manner as the plug flow equations, for several reasons:

1. An initial value for $X_B(0)$ is not available.
2. Equation (15) predicts that X'_B is directly related to X''_B. If X''_B becomes positive, this correction will increase X'_B, thus increasing X''_B, and thus X_B increases very rapidly. The solution soon gets out of hand when using a numerical stepping procedure.
3. In Eq. (21) the value of the denominator $(Q^f - Q)$ is initially very small, and thus the value obtained for Y_B is extremely sensitive to even the slightest variation in X'_B or Y'_B.

An approximate solution to Eqs. (15), (16), and (21) was developed as follows. The solution to the plug flow case is used as a *first approximation.* The values of X'_B and Y'_B from this case are used to estimate the amount of diffusional flow occurring.

For diffusion on the low-pressure side we can write

$$d_B = -K_{DL} Y'_B \tag{25}$$

Inserting this in Eq. (5) we have

$$Y_B(l+h)q(l+h) - Y_B(l)q(l) + K_{DL}Y'_B(l) - K_{DL}Y'_B(l+h) = \overline{PBF} \tag{26}$$

where

$$\overline{PBF} = K_{PB}\frac{w}{t}h(P_H X_B - P_L Y_B) \tag{27}$$

$$= \text{permeated flow of component } B \text{ in the incremental element } h$$

Solving for Y_B and putting the equation in *finite-difference form*, we have

$$Y_B(i) = \frac{1}{q(i)}\{Y_B(i-1)q(i-1) + \overline{PBF} + K_{DL}[Y'_B(i) - Y'_B(i-1)]\} \tag{28}$$

A similar equation for X_B is

$$X_B(i) = \frac{1}{Q(i)}\{X_B(i-1)Q(i-1) + K_{DH}[X'_B(i) - X'_B(i-1)] - \overline{PBF}\} \tag{29}$$

Equations (28) and (29) can be used to calculate X_B and Y_B by a

stepping procedure using values for X'_B, Y'_B, and Q from the previous approximation. Since the effect of diffusion flow is to reduce the magnitude of X'_B and Y'_B, the values for X'_B and Y'_B from the plug flow case will probably be too large. This problem will be avoided by using a diffusion constant arbitrarily chosen to be a given fraction, say 0.2, of the actual constant. This fraction will then be gradually increased in successive approximations until the full value of the diffusion constant is reached.

Equations (28) and (29) will give sharp discontinuities and X'_B values less than zero when used at the boundaries. This is because $X'_B(0)$ and $X'_B(L)$ are definitely not zero in the plug flow case. This problem will be circumvented as follows. At the feed end of the cell $X_B(1)$ will be calculated using Eq. (29) with $X'_B(0) = 0$. This will give an $X_B(1)$ value somewhat larger than the $X_B(1)$ value in the plug flow case. Since $X'_B(0) = 0$, it would be reasonable to set $X_B(0) = X_B(1)$. Therefore $X_B(0)$ will be larger than X^f_B. See Fig. 2, where A indicates the newly calculated $X_B(0)$ value. If we then calculate successive points using Eq. (29), X'_B will be negative between points $i = 1$ and $i = 2$. To avoid this, we search for an X_B

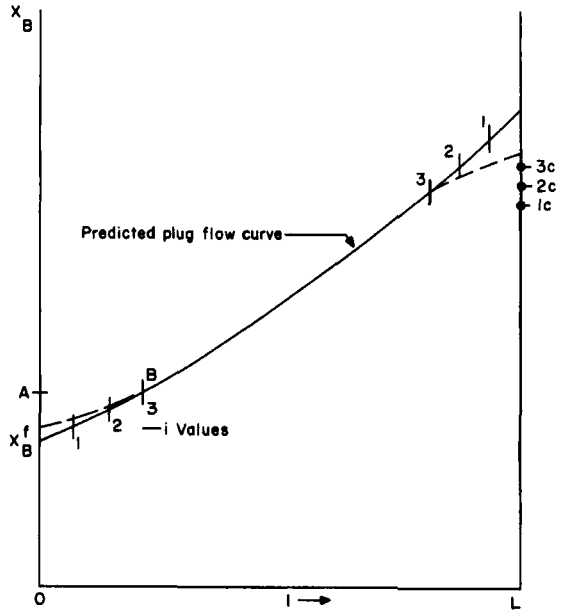

FIG. 2. Graphic aid, diffusion-mixing solution.

which is greater than $X_B(0)$. After finding X_B at point B, Fig. 2, we linearize X'_B from this point back to zero:

$$X'_B = Al \tag{30}$$

$$X_B = Al^2 + C \tag{31}$$

where C is the intercept. This procedure will give the dashed curve shown in Fig. 2 (left side).

At the product-takeoff end of the cell, a similar procedure will be followed. Using Eq. (29) we solve for $X_B(i)$ with $X'_B(i) = 0$. This will give an $X_B(i)$ value less than $X_B(i-1)$ (see Fig. 2, point 1c). If we increase the size of the increment h, the difference, $X_B(i) - X_B(i-1)$, will become smaller. (Fig. 2, point 2c), and if we increase h enough, $X_B(i)$ will be larger than $X_B(i-1)$, making X'_B positive (Fig. 2, point 3c). Again we linearize X'_B from point 3 to L, giving the dashed curve in Fig. 2 (right side).

This procedure still leaves a discontinuity in the X_B curve at points B and 3, Fig. 2. These can be removed by observing that the resultant curve closely approximates the portion of a cubic equation between the zero derivative points. A cubic equation satisfying the boundary conditions is

$$X_B = \frac{-2C}{3L} l^3 + Cl^2 + D \tag{32}$$

where C and D are constants to be determined. A least-squares technique can be used to determine these constants.

In practice the procedure of first rounding the ends of the curve can be omitted, and the plug flow curve fitted directly to Eq. (32). This simplifies the calculations somewhat and gives the same results. However, the theoretical basis for the fit of the cubic equation curve still lies in the initial rounding of the end portions of the X_B curve.

The same technique can be used on the Y_B curve, and again the least-squares cubic equation fit can be used directly without going through the intermediate steps.

The iteration procedure given in Table 2 is then used for an approximate solution to Eqs. (15), (16), and (21).

The curve-fitted $X_B(L)$ and $Y_B(L)$ values from the last iteration in Table 2 will not satisfy a total material balance exactly, owing to slight errors in the curve fit. This can be corrected as follows.

TABLE 2

Iteration Procedure for Diffusional Mixing

Given: (a) Solution to plug flow equation (Table 1)
(b) Diffusion constants K_{DH} and K_{DL}
(c) Allowable error for stopping interation

Steps in *computer use:*

(1) Use plug flow solution as first approximation
(2) Fit the resulting X_B vs. l values to the curve:

$$X_B: \frac{-2C}{3L} l^3 + Cl^2 + D$$

Fit a similar curve for the Y_B values:

(3) With an arbitrary fractional diffusion constant, calculate X_B and Y_B from Eqs. (28) and (29) using X'_B, Y'_B, and Q values from the curve fit of step (2)
(4) Increase the diffusion constant gradually, and repeat steps (2) and (3)
(5) After the diffusion constant has been increased to its actual value, iterate steps (2) and (3) until the change in $X_B(L)$ and $Y_B(L)$ between iterations is less than an allowable error

Define a theoretical X^f (denoted TX^f):

$$TX^f = X^o(L)(1 - F) - Y^p(L)F \tag{33}$$

Also, define a curve-fit error ($\overline{\text{CFE}}$):

$$\overline{\text{CFE}} = X^f - TX^f \tag{34}$$

Then set

$$X^o(L) = X^o(L)\,(\text{curve fit}) + \overline{\text{CFE}} \tag{35}$$

$$Y^p(L) = Y^p(L)\,(\text{curve fit}) + \overline{\text{CFE}} \tag{36}$$

The resulting values of $X^o(L)$ and $Y^p(L)$ satisfy a material balance exactly. The magnitude of $\overline{\text{CFE}}$ in actual computation averaged approximately 0.001 mole fraction.

For most cases, this iteration procedure converges rapidly, usually requiring no more than four or five iterations with the actual diffusion constant. For those cases where the plug flow X_B vs. l curve is significantly concave downward, the solution diverges. Results of theoretical calculations show that the difference between the predicted outlet concentrations for plug flow and for diffusion-

mixing approaches zero as X_B' approaches zero. In addition, if the diffusion-mixing solution diverges, the plug flow solution gives as good an agreement with experimental results as was obtained for cases where the diffusion-mixing solution converged. This might have been anticipated, since X_B vs. l curves which are significantly concave downward have a very small slope for a substantial portion of the cell length at the outlet end.

APPARATUS AND PROCEDURE

Rectangular barriers of microporous Vycor glass ($7\frac{11}{16} \times 2\frac{3}{8} \times 0.053$ in.) and Stauffer SS-823-RTV silicone rubber ($70 \times 4 \times 0.031$ in.) were used. Metal cells were constructed to support the barriers and to allow for sampling of the gas stream directly above and below the barriers at regular intervals. Sampling was done with a gas-tight syringe and samples were analyzed with a gas chromatograph. Six samples of each of the feed stream, the nonpermeated stream, and the permeated stream were taken and averaged. One sample was taken from each sample port above and below the barrier. When sampling the gas stream above and below the barrier, the needle of the sampling syringe was placed as close to the barrier surface as possible without damaging the needle or the barrier. However, even with a small sample size (0.5 ml), only an average of the concentration in the gas space above the barrier could be obtained. Samples were not taken below the barrier for runs where the downstream pressure was subatmospheric, as the gas syringe sampling procedure was not readily adaptable to subatmospheric sampling. The flow rates of the permeated and nonpermeated streams were measured using a soap-bubble flow meter.

RESULTS

A total of 113 experimental separation runs were made. All runs where the material-balance deviation was greater than 3% were rejected. This procedure rejected four runs. The Vycor barrier was used with He-N_2 and He-CO_2 gas mixtures and the silicone rubber barrier with a N_2-CO_2 mixture. The pressure ratio P_L/P_H was varied from 0.02 to 0.50, the cut or fraction permeated from 0.05 to 0.95, and the feed composition from 0.25 to 0.75 mole fraction of B component.

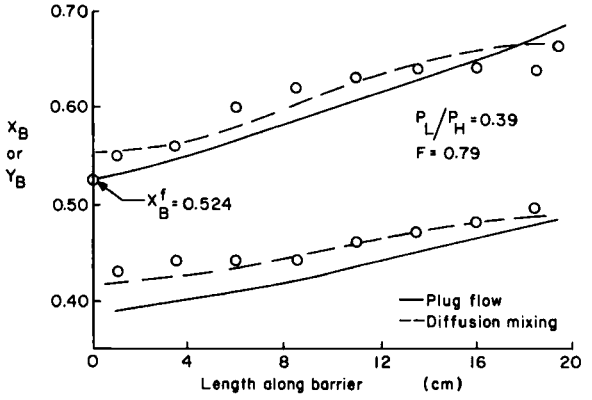

FIG. 3. Sample concentration profile, He-N_2, Vycor barrier.

Three sample profiles are given in Figs. 3, 4, and 5. The lines drawn through the points are those predicted by the plug flow model (solid lines) and the diffusion-mixing model (dashed lines). A diffusion-mixing prediction is not given in Fig. 5, as the solution diverged in this case. It can be seen however, that the plug flow model adequately predicts the *outlet* concentrations in this case.

For judging the adequacy of the theoretical models, an average absolute error in concentration prediction ($\overline{AAE}$-C), was defined as follows:

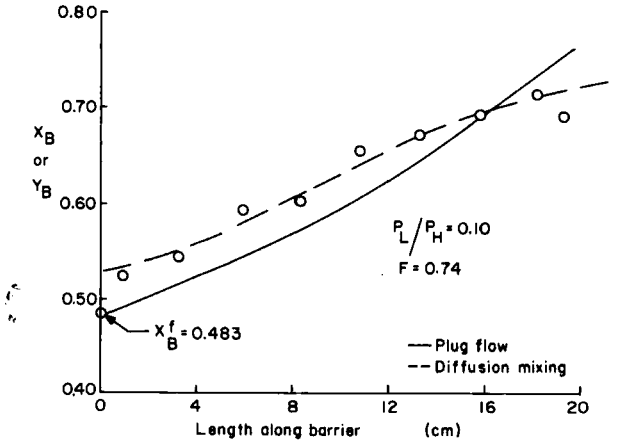

FIG. 4. Sample concentration profile, He-N_2, Vycor barrier.

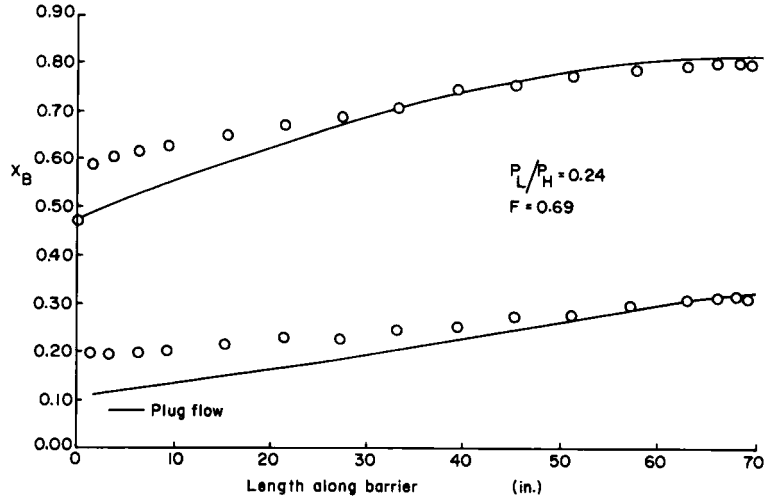

FIG. 5. Sample concentration profile, N_2-CO_2, silicone rubber.

$$X_B^Q(\%\text{ error}) = \frac{[X_B^Q(\text{predicted}) - (X_B^Q(\text{expt.})] \times 100}{X_B^Q(\text{expt.})} \tag{37}$$

$$Y_B^P(\%\text{ error}) = \frac{[Y_B^P(\text{predicted}) - Y_B^P(\text{expt.})] \times 100}{Y_B^P(\text{expt.})} \tag{38}$$

$$\overline{\text{AAE}}\text{-}C = 0.5[|X_B^Q(\%\text{ error})| + |Y_B^P(\%\text{ error})|] \tag{39}$$

where: $\overline{\text{AAE}}$-C = average absolute error in concentration prediction.

Similarly, an error for permeated flow predictions, $\overline{Eq}^P$, was defined:

$$\overline{Eq}^P = \frac{|[q^P(\text{predicted}) - q^P(\text{expt.})]| \times 100}{q^P(\text{expt.})} \tag{40}$$

The values of $\overline{\text{AAE}}$-C and $\overline{Eq}^P$ averaged for all the runs are given in Table 3. Also listed in Table 3 is the percentage of runs for which a given model predicted an X_B^Q higher than the experimental X_B^Q, and a similar value for q^P. Ideally, this value should be 50%, because if a model were perfect, one would expect the experimental points to be high one-half the time. The percentage values in Table 3 show

TABLE 3

Correlation of Theoretical Models and Experimental Data

Model	Average $\overline{AAE}$-C	Average $\overline{Eq^p}$	High predictions, %
Concentration predictions			
WS I	3.36		16
WS II	4.31		84
N-B	4.55		88
Plug flow	3.43		81
Diffusion mixing	2.39		67
Permeated flow predictions			
WS I		2.83	27
Plug flow		2.38	50
Diffusion mixing		2.27	40

the Naylor-Backer, Weller-Steiner case II, and plug flow predictions to be consistently high, whereas the Weller-Steiner case I values are usually low. Only the diffusion-mixing model approaches the ideal 50% value.

The difference in the predicted quantity of permeated flow of the different models is not nearly as pronounced as in the concentration predictions, and it is difficult to say whether there is a significant difference in the three models tested. However, the diffusion-mixing and plug flow models do approach more closely the ideal 50% high predictions than the Weller-Steiner case I model.

CONCLUSIONS

Concentration gradients in gas mixture barrier separation cells were measured, using both microporous and polymeric barriers. The interpretation of these gradients was performed while considering the available theoretical models.

Existing theories in the literature were deemed inadequate for the following reasons:

1. The theories which assume perfect mixing predict a uniform concentration, i.e., no gradient, on both high- and low-pressure sides of the cell. The existence of a gradient indicates that the perfect mixing assumption is invalid.

2. The theories which supposedly assume no mixing actually assume that the barrier is far enough away from the low-pressure flow stream that the gas composition of this stream does not affect

the composition next to the barrier. Since this will not normally be the case, this assumption is also invalid.

A two-part theoretical model was developed in this study. In the first part, plug flow, i.e., unidirectional flow, is assumed. This is essentially a no-mixing theory which allows for both high- and low-pressure flow streams to be adjacent to the barrier. In the second part, diffusional flow caused by the concentration gradient is taken into account. A straightforward numerical solution to the plug flow model has been developed. An approximate solution for the model involving diffusional flow has been proposed. The plug flow equations are solved and then a correction factor involving diffusion is added to the plug flow solution. This iterative approximate solution converges in most cases.

The proposed model represents the experimental data in this study more adequately than any of the previous models. Given the feed concentration, feed flow rate, barrier and cell geometry, and permeability and diffusion coefficients, this model will give predictions for the concentration gradient on both the high- and low-pressure sides of the cell. It also yields predictions of both permeated and nonpermeated outlet concentrations, and the permeated flow rate. Where the iterative solution to the diffusion mixing model does not converge, the model does not adequately predict the concentration profile, but it still gives adequate predictions for outlet conditions.

Nomenclature

$\overline{\text{AAE-C}}$	average absolute error in concentration prediction, %
$\overline{\text{CFE}}$	curve-fit error
d	diffusion flow, low-pressure side of barrier
D	diffusion flow, high-pressure side of barrier
D	diffusion coefficient
$\overline{\text{DPA}}$	partial pressure difference, A component
$\overline{\text{DPB}}$	partial pressure difference, B component
$\overline{Eq^P}$	error in permeate flow prediction, %
F	fraction of feed permeating barrier
h	length of incremental element
K	constant
l	length
L	total length of cell
P	pressure

$\overline{PBF}$	permeated flow of component B in incremental element
q	flow rate, low-pressure side of barrier
Q	flow rate, high-pressure side of barrier
t	thickness
TX^f	"theoretical" X^f
w	width
X	mole fraction, high-pressure side of barrier
Y	mole fraction, low-pressure side of barrier
X'	dX/dl
X''	d^2x/dl^2

Subscripts:

A	component A of mixture
B	component B of mixture
D	diffusion
H	high-pressure side
L	low-pressure side
P	permeability

Superscripts:

f	feed stream
O	high-pressure outlet
P	low-pressure outlet

Acknowledgment

The authors wish to acknowledge the financial support of the National Science Foundation for this research.

REFERENCES

1. D. W. Brubaker and K. Kammermeyer, *Ind. Eng. Chem.*, **44**, 1465 (1952).
2. H. E. Huckins and K. Kammermeyer, *Chem. Eng. Progr.* **49**, 294 (1953).
3. K. B. McAfee, Jr., *Encyclopedia of Chemical Technology*, 2nd suppl. vol. (R. E. Kirk and D. F. Othmer, eds.), Wiley-Interscience, New York, 1960, p. 302.
4. R. W. Naylor and P. O. Backer, *A. I. Ch. E. J.*, **1**, 95 (1955).
5. J. Oishi, Y. Matsumura, K. Higashi, and C. Ike, *J. At. Energy Soc. Japan*, **3**(12), 923 (1961).
6. S. A. Stern, et al., *Ind. Eng. Chem.*, **57**, 49 (1965).
7. S. Weller and W. A. Steiner, *J. Appl. Phys.*, **21**, 279 (1950).
8. S. Weller and W. A. Steiner, *Chem. Eng. Progr.*, **46**, 585 (1950).

Received by editor February 20, 1967
Submitted for publication March 14, 1967